A DFT analysis of the ground and excited states electronic structure of Sc_3N@Ih-C_{80} fullerene coupled with metal-free and Zinc-phthalocyanine

Journal:	*Physical Chemistry Chemical Physics*
Manuscript ID	CP-ART-06-2018-003849.R1
Article Type:	Paper
Date Submitted by the Author:	10-Sep-2018
Complete List of Authors:	Amerikheirabadi, Fatemeh; University of Texas at El Paso, Computational Science Program Diaz, Carlos; University of Texas at El Paso Mohan, Neetha; University College London Department of Chemistry, Department of Chemistry Zope, Rajendra; University of Texas at El Paso, Physics Baruah, Tunna; University of Texas at El Paso, Physics

A DFT Analysis of the Ground and Charge-transfer Excited States of $Sc_3N@I_h$-C_{80} fullerene coupled with metal-free and zinc-phthalocyanine

Fatemeh Amerikheirabadi[1,2], Carlos Diaz[1], Neetha Mohan[2], Rajendra R. Zope,[1,2] and Tunna Baruah[1,2a)]

[1]*Computational Science Program, The University of Texas at El Paso, El Paso, Texas, 79968, USA*

[2]*Department of Physics, The University of Texas at El Paso, El Paso, Texas, 79968, USA*

ABSTRACT

Endohedral metallofullerenes and phthalocyanine derivatives are recognized as excellent active materials in organic photovoltaics (OPVs). The tri-metallic nitride endohedral C_{80} fullerenes have greater absorption coefficients in the visible region and electron-accepting ability similar to C_{60} which can allow for higher efficiencies in OPV devices. In this work, we have investigated the ground and charge transfer excited states of two co-facial donor-acceptor (D–A) molecular conjugates formed by non-covalent coupling of trimetallic nitride endohedral fullerene ($Sc_3N@I_h$-C_{80}) with metal-free (H_2Pc) and zinc-phthalocyanine (ZnPc) chromophores using DFT calculations. The charge transfer (CT) excitation energies are calculated using perturbative delta-SCF method that enforces orthogonality between the ground and excited states. The binding energies calculated using PBE and DFT-D3 method indicates that the dispersion effects play an important role in the stabilization of these complexes. The ground state dipole moment of $Sc_3N@C_{80}$-H_2Pc dyad is much larger than that of $Sc_3N@C_{80}$-ZnPc, but this is reversed in the excited state where the dipole moment of $Sc_3N@C_{80}$-ZnPc increases significantly. The lowest few excitation energies in gas phase for the two complexes are very close in the range of 1.51 – 2.66 eV for the $Sc_3N@C_{80}$-ZnPc and 1.51 – 2.71 eV for the $Sc_3N@C_{80}$-H_2Pc complex. However, low ionization potential and low exciton binding energy make $Sc_3N@C_{80}$-ZnPc dyad a better candidate for OPVs compared to $Sc_3N@C_{80}$-H_2Pc dyad.

I. INTRODUCTION

Organic photovoltaics (OPVs) represent a class of cost-effective, lightweight solar energy conversion technology for long term sustainable energy production, that has attracted much scientific attention in recent years[1-3]. Substantial progress has been made in increasing the power conversion efficiencies of OPVs by the development of novel donor-acceptor (D–A) blends, utilization of new device architectures, and the use of interfacial materials for improved charge-carrier collection[3-7]. However, the power conversion efficiency of OPVs are still much smaller than their inorganic counterparts owing to poor material properties like low charge carrier mobilities, poor band offsets and low dielectric constants[8]. It is well established that open circuit voltage (V_{OC}) in OPVs is linearly dependent on the energetic

a) **Author to whom correspondence should be addressed. Electronic mail: tbaruah@utep.edu**

difference between the Highest Occupied Molecular Orbital (HOMO) of the donor and Lowest Unoccupied Molecular Orbital (LUMO) of the acceptor *viz*., the donor-acceptor effective energy gap[9-14]. In general, only a small fraction of the incident solar irradiation is harvested by the organic materials due to their large band gaps. Consequently, alignment of LUMO and HOMO levels of donor and acceptor plays a crucial role in determining the performance of solar cells. Hence, increasing open circuit voltage by choosing efficient and appropriate D-A pairs is a relevant and active area of research.

Metal containing endohedral fullerenes or endohedral metallofullerenes (EMF) have attracted particular interest as electron acceptors in D–A dyads due to their unique structure and properties[15, 16]. Apart from their higher absorption coefficients in the visible region and low reorganization energies, the ability to fine tune their HOMO−LUMO gaps by varying the nature and composition of the encapsulated species make them excellent candidates as electron acceptors[17, 18]. Since the discovery of a trimetallic nitride template endohedral metallofullerene by Stevenson et al. in 1999[19], a variety of other endohedral families with different types of endohedral units have been synthesized and characterized. EMFs of the type $M_3N@C_{80}$ (M = Sc, Y, Gd, Tb, Dy, Ho, Er, Tm, Lu), possess reduced donor/acceptor LUMO offset and hence offer the possibility of dramatically increasing the power conversion efficiency[20]. The stability and unusual reactivity of nitride EMFs is explained using an ionic model that considers a charge transfer of up to six electrons from the endohedral species to the carbon cage, leading to a $(M_3N)^{6+}@(C_{2n})^{6-}$ species. Ross et al.[20, 21] cleared a path towards higher power conversion efficiencies in OPV devices by synthesizing $Lu_3N@C_{80}$ and incorporating its derivative, phenyl-$Lu_3N@C_{81}$ butyric hexyl ester (also known as $Lu_3N@C_{80}$–PCBH), as acceptor in a P3HT/$Lu_3N@C_{80}$ – PCBH device with an V_{OC} of 890 mV, the highest reported V_{OC} for any P3HT-fullerence device. This work initiated the development of a series of covalently linked D–A systems containing conjugates of endohedral fullerenes with a myriad of acceptors such as ferrocenes, triphenylamines, porphyrins, corroles and tetrafulvalenes[22-28]. Non bonding interactions like hydrogen bonding[29-31], electrostatic interactions[32], π-π stacking[33-35] and metal coordination[36] have also been efficiently utilized as an excellent alternative to covalent approach for the construction of novel functional electron D–A systems. For instance, the radical ion pair viz., $(ZnPc)^{\cdot+}$–$(C_{60})^{\cdot-}$ in ZnPc/C_{60} D–A architecture formed by biomimetic organization principles[37] has been found to be about three orders of magnitude longer-lived compared to similar covalently linked ZnPc–C_{60} conjugates[38]. More recently, several examples of EMF based D–A conjugates have been reported where the EMF acts as an electron donor when covalently linked to electron accepting moieties like tetracyanoanthraquinodimehane[39], perylene-diimides[40, 41] and subphthalocyanines[42]. A very recent report by Guldi *et al*[43] highlights the amphoteric nature of EMFs, acting both as electron-acceptor or electron-donor, where the activation of oxidative and/or reductive electron-transfer reactions is simply by the electronic nature of its counterpart.

Owing to their outstanding electronic and photophysical properties, fullerene derivatives as electron accepting units in combination with porphyrin/phthalocyanine derivatives as electron donors appear particularly promising. Phthalocyanines (Pcs) are highly π-conjugated

porphyrin analogs that are capable of binding a variety of transition metals within its central cavity, thus leaving the axial positions axial available for binding with a variety of ligands. Bruder et al.[44] examined a series of bilayer heterojunction solar cells employing C_{60} as n-conducting and CuPc, FePc, NiPc or ZnPc, as p-conducting organic layers and identified the ZnPc based device as the best performing metal phthalocyanines among their probed cells. Recently, Wolfrum et al[45] showed that electron transfer reactions between ZnP as an electron donor, and $Sc_3N@C_{80}$ as an electron acceptor promotes long-range charge transfer events with lifetimes in the range of microseconds. This is longer than most other organic dyads or solar cells where the exciton lifetimes range from picosecond to nanosecond range. However, extra long lifetimes from seconds to days also have been achieved through multistep charge transfer processes in supramolecular structures with several components.[46-49] These recent experiments have shown that through careful rational design it is possible to achieve very long lifetimes comparable to that in bacterial photosynthetic centers.

In a previous work[50], we carried out DFT calculations on the ground and excited states electronic structure of two D–A complexes in which $Sc_3N@C_{80}$ and $Y_3N@C_{80}$ molecules were coupled with Zn-tetraphenyl porphyrin (ZnTPP) and showed that the charge transfer excited state energies of endohedral fullerene-ZnTPP dyads are larger than those of C_{60}-ZnTPP and C_{70}-ZnTPP dyads. In this work, we study the electronic and charge transfer excited state properties of D–A dyads made by pairing $Sc_3N@C_{80}$ with two members of phthalocyanine (Pc) family viz., free base (H_2Pc) and zinc-phthalocyanine (ZnPc). The ZnPc has been used in organic photovoltaics but in this study we also include H_2Pc to understand the role of the metal center in the phthalocyanine. The photovoltaic properties of H_2Pc was recognized decades ago[51,52]. Photovoltaics properties of H_2Pc with C_{60} shows strong structural effects [53,54]. The CT excitation energies are calculated using our perturbative delta-SCF method that has been shown to be a reliable approach for this purpose. The effect of changing the donor component on the ground state and excited state electronic structure of the D-A dyads with $Sc_3N@C_{80}$ as acceptor is analyzed.

II. COMPUTATIONAL METHOD

The geometry optimization of the isolated $Sc_3N@I_h$-C_{80} and ZnPc/H_2Pc molecules as well as the $Sc_3N@C_{80}$-ZnPc/H_2Pc complexes are performed at all-electron level using Perdew-Burke-Ernzerhof[47] (PBE) exchange correlation function using the NRLMOL code [56-59]. We have employed icosahedral C_{80} or I_h-C_{80} for the calculations since it has been reported as the most stable isomer of the outer C_{80} cage among various $Sc_3N@C_{80}$ isomers[17]. The Sc_3N unit in the $Sc_3N@I_h$-C_{80} interacts with the icosahedral C_{80} cage through ionic interactions and can rotate freely within the C_{80} cage. Five different orientations of Sc_3N cluster in the icosahedral cage have been reported previously by Dorn et al[60]. We have used an arbitrary orientation of the Sc_3N with respect to the plane of ZnPc or H_2Pc for the calculations, since our previous work[50] indicated that the orientation of the endohedral unit does not significantly affect the CT state energies. The NRLMOL default basis set, optimized for PBE exchange-correlation energy functional, is used for all the calculations. It has been shown to correctly satisfy the $Z^{10/3}$ rule for Gaussian basis sets, where Z is the atomic number, so that the basis set

superposition errors are minimized[61]. The binding energies of the complexes are calculated using the supermolecular approach i.e., interaction energy of the complex = energy of the complex – energy of the reactants optimized separately.

Here, the binding energy, $E_{BE} = E_{Sc3N@C80\text{-}ZnPc/H2Pc} - (\sum E_{ZnPc/H2Pc} + E_{Sc3N@C80})$.

Since the complexes are bound by van der Waals interactions, DFT-D3 parameters[62] with Becke–Johnson damping model as implemented in NRLMOL code is used for calculating the binding energies. The vertical ionization energies (vIE) are calculated as the energy difference between the neutral molecule and positively charged molecule while electron affinities (vEA) are calculated as the energy difference between the neutral molecule and negatively charged molecule where the molecular geometry of the two states are the same. The quasi-particle gap (QP) is calculated from the difference between ionization potential and electron affinities thus calculated and the exciton binding energy (EBE) is calculated as the difference between the quasi-particle gap and the optical gap where the optical gap is the same as the HOMO-LUMO excitation energy.

The charge transfer excited states are obtained using perturbative delta-SCF method [63,64] which is a variant of the standard delta-SCF approaches. Delta-SCF approximation places one or more electrons in high lying Kohn-Sham orbitals, instead of placing all electrons in the lowest possible orbitals as one does while calculating ground state energy in standard DFT calculations. Perturbative delta-SCF method, developed in our lab and implemented in NRLMOL code, enforces an orthogonality constraint between the ground state and excited state determinantal wave functions. In this method, the occupied orbitals are relaxed using the first order perturbation method where the perturbation Hamiltonian is the change in the ground state Hamiltonian due to rigid shift of an electron from the hole to the particle orbital. The occupied orbitals are relaxed in the space of unoccupied orbitals while the hole orbitals are relaxed in the space of occupied orbitals. This constraint enforces the strict orthogonality between the ground and excited state wavefunctions. Perturbative delta-SCF method has been shown to accurately describe CT excitations of several molecular D–A dyads and triads [65,66]. Furthermore, previous benchmark calculations[50] on a set of small D–A pairs have shown that this method in conjunction with pure GGA functional can yield results with accuracy comparable to those of TDDFT method employing range-separated functionals. The charge transfer excitation energy for the donor–acceptor complexes is estimated using the Mulliken's formula[67] as IE − EA − 1/R within the point charge approximation, where IE and EA are the ionization potential of the donor and electron affinity of the acceptor, respectively and R is the particle-hole separation. The 1/R term is the Coulomb energy originating from the electrostatic interaction between the charged donor and acceptor species.

All the calculations performed here are in gas phase, although in practice the D–A pairs are placed in a solvent like toluene, chloroform or benzonitrile. It may be noted that the excitation energies may change slightly due to polarization effects in solution or in aggregated form.

III. RESULTS AND DISCUSSION

The dyads studied in this work are in co-facial orientation and are bound together by van der Waals interactions. $Sc_3N@I_h$-C_{80} is the most abundant metallo-fullerene obtained as a single isomer and can be readily purified by non-chromatographic methods. The optimized geometry of $Sc_3N@I_h$-C_{80} displays a trigonal planar geometry for the entrapped Sc_3N cluster similar to the available experimental reports. The icosahedral cage of $Sc_3N@C_{80}$ has a radius of 4.11 Å and displays two types of C–C bonds viz, the 5:6 bonds, abutted by a hexagon and a pentagon and the 6:6 bonds, abutted by two hexagons. The average bond lengths for the 5:6 and 6:6 bonds are found to be 1.45 and 1.43 Å, respectively while the average Sc-N bond length is 2.04 Å. Figure 1 presents the optimized geometries of $Sc_3N@C_{80}$-ZnPc and $Sc_3N@C_{80}$-H_2Pc dyads. The smallest surface-to-surface distance between the fullerene cage and the ZnPc in the optimized geometry of the $Sc_3N@C_{80}$–ZnPc dyad is 3.17 Å and that for the $Sc_3N@C_{80}$-H_2Pc dyad is 3.16 Å. It is seen that the orientation of the endohedral Sc_3N unit is not altered in both complexes during the optimization. As mentioned in the computational methods, the binding energy of the complexes has been calculated using Becke–Johnson damping model to account for the dispersion contribution. The binding energy values are reported in Table 1. The energies of the complexes calculated at various separations show a shallow flat potential well.

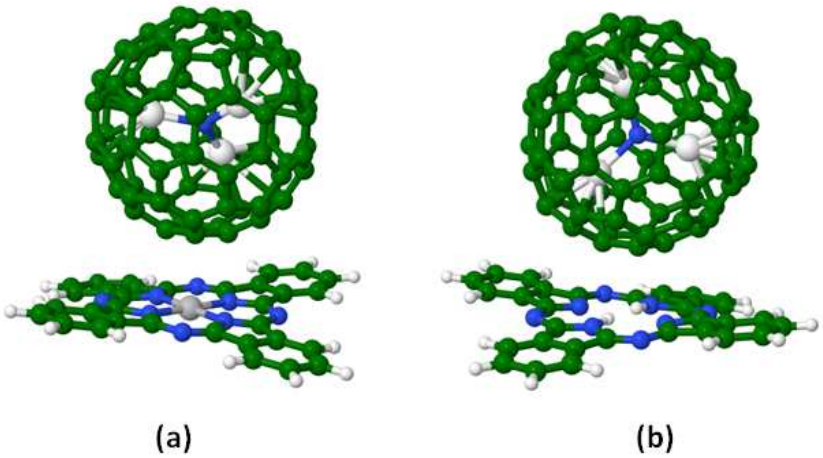

FIGURE 1. The optimized structures of (a) $Sc_3N@C_{80}$-ZnPc and (b) $Sc_3N@C_{80}$-H_2Pc dyads. The C, N, and H atoms are shown in green, blue, and white. The Sc atoms inside the cage are shown in light grey and Zn in ZnPc is shown in darker gray.

TABLE 1: The binding energies calculated using PBE functional without dispersion correction ($E_{BE}(1)$) and using DFT-D3 parameters with BJ damping ($E_{BE}(2)$), vertical ionization potential (vIP), vertical electron affinity (vEA), quasiparticle (QP) gap and exciton binding energy (EBE) of the dyads. The vEA of the fullerene donor and vIPs of the acceptors are also listed. All values in eVs.

System	E_{BE} (1)	E_{BE} (2)	vIP	vEA	QP
$Sc_3N@C_{80}$-ZnPc	-0.31	0.44	6.12	2.62	3.50
$Sc_3N@C_{80}$-H_2Pc	-0.24	0.42	6.17	2.64	3.53
$Sc_3N@C_{80}$				2.49	
ZnPc/ H_2Pc			6.35/6.39		

The complexes studied here are bound mainly due to van der Waals interaction. The calculated binding energies at the PBE level of approximation and that with inclusion of van der Waals interaction are presented in Table 1. It is evident that dispersion plays an important role in stabilization of dyads. The binding energies for the $Sc_3N@C_{80}$-ZnPc and $Sc_3N@C_{80}$-H_2Pc dyads are 0.44 eV and 0.42 eV, respectively at the DFT-D3 level. The binding energies indicate slightly greater stabilization of the dyad with zinc coordinated phthalocyanine donor compared to the one with free-base phthalocyanine donor.

The DFT calculated vertical ionization potential (vIP), vertical electron affinity (vEA) of these two systems along with their isolated components are reported in Table I. The calculated electron affinity $Sc_3N@C_{80}$ at the PBE level is 2.49 eV which differs by ~0.32 eV from the experimental electron affinity reported by Ioffe and coworkers[70]. Using the Knudsen cell mass spectrometry ion-molecular equilibria method, Ioffe et al. reported the experimental electron affinity of $Sc_3N@C_{80}$ in the gas-phase to be 2.81 ± 0.05 eV at a temperature range of 914-1016 K. The discrepancy between the experimental and the calculated values might be due to the fact that the experimental measurements are performed at high temperature while our calculations are performed at T = 0 K. Further, as reported in our previous study[50], the use of different density functionals can result in variation of the electron affinity by as much as 0.6 eV, with a general trend that inclusion of Hartree–Fock exchange leads to a reduction in its value. The present methodology accurately predicts the electron affinities of C_{60} and C_{70} fullerenes (Refs. 64-66). The calculated vertical ionization potentials for ZnPc and H_2Pc are 6.35 and 6.39 eV, respectively which are in close agreement with the results of gas-phase photoelectron spectra experiments[71] for the vertical ionization potentials of ZnPc (6.37 eV) and H_2Pc (6.41 eV). A comparison of the vIP values in the isolated donors and the D-A dyads indicates that the HOMO levels of the ZnPc and H_2Pc are raised by 0.24 eV and 0.23 eV as it couples with $Sc_3N@C_{80}$ forming the complexes. On the other hand, the LUMO of the $Sc_3N@C_{80}$ is lowered by 0.12 eV in $Sc_3N@C_{80}$-ZnPc and 0.15 eV in $Sc_3N@C_{80}$-H_2Pc. The smaller ionization potential for $Sc_3N@C_{80}$-ZnPc (6.12 eV) compared with $Sc_3N@C_{80}$-H_2Pc (6.17 eV) is in consonance with the observation by Torres *et al.*[72] that Zn-containing complexes are easier to oxidize than their Zn-free analogues. The quasi-particle gap calculated as the difference between the vIP and vEA is nearly of the same magnitude for

both $Sc_3N@C_{80}$-ZnPc and $Sc_3N@C_{80}$-H_2Pc dyads with values 3.50 and 3.53 eV, respectively (Cf. Table 1).

The HOMO-LUMO gap, calculated as difference between eigenvalues is 1.44 eV at the PBE level for isolated $Sc_3N@C_{80}$ fullerene, suggesting a noticeable chemical stability similar to C_{60}. This value is close to that obtained earlier by Zhu et al.[73] using pseudopotentials. The HOMO of $Sc_3N@C_{80}$ is spread over the C_{80} cage whereas the LUMO is spread over both the cage and the Sc_3N unit[50]. The ground state HOMO-LUMO gaps for $Sc_3N@C_{80}$-ZnPc and $Sc_3N@C_{80}$-H_2Pc complexes are 1.14 eV and 1.32 eV, respectively. However, the HOMO-LUMO gap as obtained from the Kohn-Sham eigenvalues does not present the correct corresponding excitation energies for two reasons. Firstly, because the Kohn-Sham DFT underestimates the band (fundamental) gap due to missing derivative discontinuity. This is the case even if the exact exchange-correlation functional is employed. In practical calculations, such those employed the self-interaction correction also affect the eigenvalue spectrum resulting in smaller HOMO-LUMO gap. Secondly the HOMO-LUMO gap also does not provide an estimate of optical gap as particle-hole interactions are missed [66].

Fig. 2 illustrates the ground state density of states (DOS) of $Sc_3N@C_{80}$-ZnPc and $Sc_3N@C_{80}$-H_2Pc dyads projected on their corresponding components in the left and right panels, respectively. The red line indicates the Fermi energy level that separates the occupied states on left from the unoccupied states on the right. The DOS plots show a good number of low-lying closely spaced unoccupied molecular orbitals above the LUMO level for the complexes which is inherited from the $Sc_3N@C_{80}$ molecule. The HOMO is located on the donor component viz., ZnPc or H_2Pc in both the complexes whereas the LUMO orbital localization is different in both. In $Sc_3N@C_{80}$-ZnPc, the LUMO orbital is localized solely on $Sc_3N@C_{80}$ while in $Sc_3N@C_{80}$-H_2Pc the LUMO is delocalized on both $Sc_3N@C_{80}$ and H_2Pc components. Thus, the HOMO to LUMO transition corresponds to charge transfer excited state in ZnPc complex which is in agreement with the earlier observations in $Sc_3N@C_{80}$-ZnTPP and $Y_3N@C_{80}$-ZnTPP dyads[50]. The HOMO-LUMO transition in the H_2Pc complex is the result of a partial charge transfer (since there is a non-zero overlap between the particle and the hole orbitals). Furthermore, the lowest three LUMOs (LUMO, LUMO+1 and LUMO+2) are degenerate in this dyad. Another noticeable feature of these complexes is the high lying occupied states of $Sc_3N@C_{80}$ fullerene as can be seen from the DOS plot.

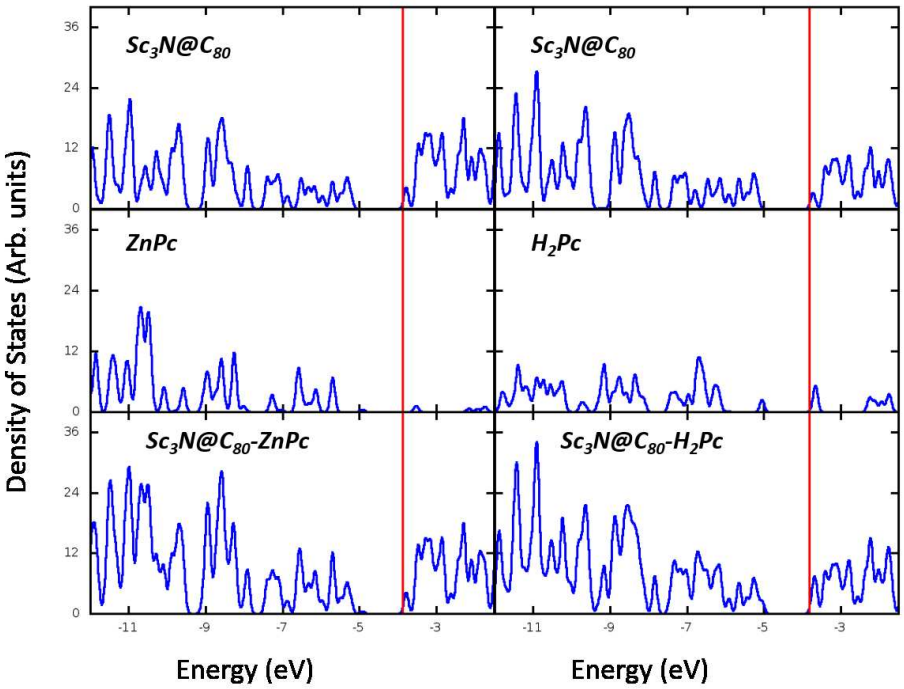

FIGURE 2. The ground state density of states of the two dyads, $Sc_3N@C_{80}$-ZnPc (left panel) and $Sc_3N@C_{80}$-H_2Pc (right panel) and the DOS projected on their corresponding components. The Fermi level is shown as a red vertical line.

An important parameter that determines the efficiency of the photovoltaic device is the open-circuit voltage which is proportional to the charge-transfer excitation energy.. Excitation energies (both singlet and triplet excited state energies of the single particle excitations) of several low-lying excited states of the $Sc_3N@C_{80}$-ZnPc and $Sc_3N@C_{80}$-H_2Pc dyads are listed in Table 2. We have carried out the calculations of the excited states corresponding to the transitions from HOMO, HOMO–1 and HOMO–2 to lowest four LUMOs. Due to the hybridization between the orbitals of the donor and acceptor moieties, there are very few states that are purely charge transfer states with nearly zero transition dipole moment. The transitions that correspond to local excitations and partial charge transfer excitations are indicated with one and two asterisks, respectively in the table. The singlet excited state energies (E_S) are calculated using the prescribed Ziegler-Rauk method[74] which determines E_S as $E_S = 2E_M - E_T$, where E_M and E_T are the excitation energies of the mixed and triplet states. The LUMO in $Sc_3N@C_{80}$ is a nondegenerate orbital whereas the next higher unoccupied orbitals have double or near degeneracies. All the indicated transitions are optically allowed with HOMO to LUMO+1 and LUMO+2 transitions having the highest probability of occurrence in both complexes. Our orthogonality constrained delta-SCF method gives the optical gap of 1.52 eV for the isolated $Sc_3N@C_{80}$. This energy corresponds to the HOMO to LUMO transitions in the fullerene which are very weak in intensity. This result is in excellent agreement with the experimentally measured optical gap of 1.51 eV by Dunsch et al. [75]

The excitations from HOMO and HOMO–1 to the lowest three LUMOs of both the complexes are also presented schematically in figures 3 and 4. In both the complexes, the HOMO is located on the phthalocyanine but the HOMO-1 and HOMO-2 are on the fullerene. Similarly, the LUMO and LUMO+3 mainly arise from the fullerene in both the complexes but the LUMO+1 and LUMO+2 are located on the phthalocyanine. The DFT calculated singlet excitation energies lie within a range of 1.51 – 2.66 eV for the $Sc_3N@C_{80}$-ZnPc complex and 1.51 – 2.71 eV for the $Sc_3N@C_{80}$-H_2Pc complex. The lowest excitation energy at 1.51 eV corresponds to excitation of the $Sc_3N@C_{80}$ in the ZnPc complex but of the H_2Pc in the H2Pc-containing complex. The energies of lowest two excited states involving significant charge transfer from ZnPc to $Sc_3N@C_{80}$-ZnPc are 1.93 and 2.14 eV. In the H_2Pc analogue, the lowest CT excitation is at 1.63 eV that corresponds to the HOMO-LUMO excitation. On the other hand, the reverse charge transfer excitations involving charge transfer from fullerene to phthalocyanine are seen at 2.20 eV and 1.93 eV for the ZnPc and H_2Pc containing complexes, respectively. Previously, Basurto et al.[50] have reported the lowest CT excitation energies for two isomers of $Sc_3N@C_{80}$-ZnTPP as 2.11 eV and 2.16 eV. Our present results suggest a lowering in the CT excitation energy as $Sc_3N@C_{80}$ fullerene couples with ZnPc/H_2Pc compared to its coupling with Zn tetraphenyl porphyrin. To check the effects of different orientations of the Sc_3N unit on the CT energies in the H_2Pc complex, we have calculated to CT energies with an orientation that is parallel to the plane of the phthalocyanine. We find that our earlier observation holds for H_2Pc complexes as well where the CT energies change on the order a few hundredths of eV (0.01-0.05 eV). Overall, the Q-band excitations of the donor moieties are unlikely to lead to charge transfer to the fullerene moiety. Higher excitations are needed to achieve charge transfer to the fullerene. Trukhina et al. have earlier prepared N-pyridyl substituted $Sc_3N@Ih$-C_{80} axially attached to ZnPc[43]. They found that electron transfer occurs from the ZnPc to the fullerene when the ZnPc is electron rich but the reverse can also happen if the ZnPc is electron deficient [43]. Their electrochemical measurements in dichlorobenzene gives an estimate of 1.20 eV or 1.81 eV for the ZnPc to fullerene charge transfer excited state for the electron-rich and electron-deficient complexes. For these systems the reverse electron transfer excited states are at 1.79 eV and 0.94 eV [43]. A direct comparison of our results with the experimental values presented in Ref. 43 is not possible since in experiment of Trikhine et al. [43] derivatives of ZnPc and $Sc_3N@C_{80}$ are used. Moreover, the solvent effects and ionic relaxations are also not accounted for in the theoretical calculations. Both of these effects tend to stabilize the energies of the charge transfer states. The relaxation of the fullerene in the anionic state is small leading to small ionic relaxation effects on the charge transfer energies. The solvent polarization effects on the other hand will be a stronger effect. The incorporation of the solvent polarization effects will be pursued in a future work.

The ground state dipole moment near the equilibrium separation of the supramolecular D–A pairs indicates the formation of interfacial dipoles, which facilitates orbital alignments that leads to better exciton dissociation. The interfacial dipole originates predominantly from polarization effects or from the ground state charge transfer from the donor to acceptor. The ground state charge transfer reduces as the D–A components get farther away and makes the polarization effect entirely responsible for the dipole formation at large separations[65]. Based

on experimental reports[68] on the co-sublimated thin films of ZnPc and C_{60} at room temperature, the ground state shows to be an intrinsic charge transfer state with partial charge transfer from ZnPc moiety to C_{60}, whereas some other experiments[69] claim no evidence of ground state charge transfer in C_{60}-H_2Pc system. Our calculated dipole moments for $Sc_3N@C_{80}$-ZnPc and $Sc_3N@C_{80}$-H_2Pc complexes are 0.32 and 1.4 Debye, respectively. The dipole moment tends to approach zero as the fragments of the dyads get farther away from each other. Although it is observed that the ground state dipole moment of the $Sc_3N@C_{80}$-H_2Pc complex is nearly four times larger than the other dyad, this is interestingly reversed in the excited state involving HOMO to LUMO transition as dipole moment values are increased to 23.5 D and 8.7 D for the fullerene-ZnPc/H_2Pc complexes, respectively. This can be explained by the fact that an overlap is observed between the hole and particle orbitals in excited $Sc_3N@C_{80}$-H_2Pc dyad corresponding to HOMO-LUMO transition for which the dipole moment values are reported.

Earlier experimental investigations[76] on a series of D–A complexes using C_{60} and C_{70} as acceptors and tetra-tert-butylphthalocyanine (H_2TBPc) and its zinc derivative (ZnTBPc) as donors in solution, have suggested higher efficiencies for electron transfer from ZnTBPc to C_{60} (or C_{70}). However, the lifetimes of the ion radicals of C_{60}-H_2TBPc and C_{70}-H_2TBPc compounds have been shown to be longer than those of C_{60}-ZnTBPc and C_{70}-ZnTBPc. A similar observation has been made by Guldi et al.[38] in their studies on C_{60}-ZnPc (or H_2Pc) dyads. Although the calculated excitation energies tabulated in Table II seem to be very close for the two dyads, we should keep in mind that there are many other factors contributing to the overall performance of OPVs. The exciton binding energies for the lowest CT transitions from phthalocyanine to fullerene in ZnPc and H_2Pc dyads are 1.57 and 1.90 eV respectively (Table 1). The higher exciton binding energy of $Sc_3N@C_{80}$-H_2Pc dyad makes the charge separation step more challenging making it a less favorable candidate. As discussed before, the ionization potential for ZnPc dyad is smaller. This makes the oxidation step easier for this dyad compared with $Sc_3N@C_{80}$-H_2Pc. Thus from all the above mentioned facts viz, the smaller ionization potential, low exciton binding energy and the available experimental results, we expect a better cell performance for the dyad employing ZnPc as the donor moiety.

TABLE II: The lowest four singlet CT excitation energies of $Sc_3N@C_{80}$-ZnPc and $Sc_3N@C_{80}$ H_2Pc dyads. The single stars refer to partial CT and double star excitations refer to the local excitations. The energies of the triplet states are given in parentheses. All energies are in eV.

Transition	$Sc_3N@C_{80}$-ZnPc (eV)	$Sc_3N@C_{80}$-Pc (eV)
HOMO → LUMO	2.14(2.12)	1.63(1.49)**
HOMO → LUMO+1	1.56(1.37)**	1.51(1.26)*
HOMO → LUMO+2	1.55(1.31)*	1.52(1.31)*

HOMO → LUMO+3	1.93(1.82)	2.71(2.70)
HOMO-1 → LUMO	1.51(1.46)*	1.52(1.48)**
HOMO-1 → LUMO+1	2.66(2.35)**	2.37(2.35)
HOMO-1 → LUMO+2	2.20(2.20)	1.93(1.90)
HOMO-1 → LUMO+3	1.90(1.87)*	1.89(1.86)*
HOMO-2 → LUMO	1.60(1.55)*	1.61(1.56)**
HOMO-2 → LUMO+1	2.19(2.16)**	2.48(2.46)
HOMO-2 → LUMO+2	2.46(2.44)	2.04(2.01)
HOMO-2 → LUMO+3	1.99(1.94)*	1.97(1.92)*

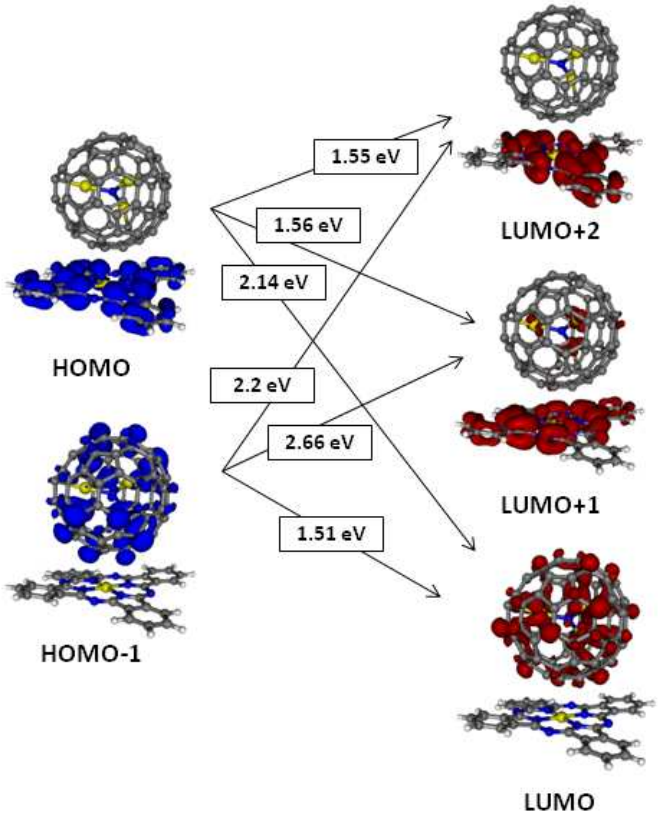

FIGURE 3. The CT transitions from HOMO and HOMO − 1 to lowest three LUMOs of $Sc_3N@C_{80}$-ZnPc dyad. The orbitals densities of the active orbitals are shown.

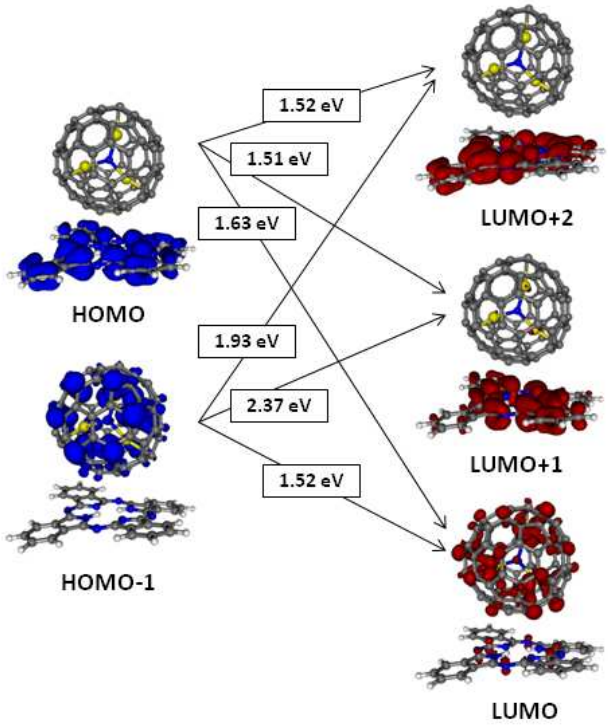

FIGURE 4. The CT transitions from HOMO and HOMO − 1 to lowest three LUMOs of $Sc_3N@C_{80}$-H_2Pc dyad. The orbitals densities of the active orbitals are shown.

In summary, we have studied the ground and excited state electronic properties of two non-covalently bound co-facial D–A molecular conjugates, $Sc_3N@C_{80}$-ZnPc and $Sc_3N@C_{80}$-H_2Pc in which $Sc_3N@C_{80}$ fullerene acts as acceptor and Zn-phthalocyanine (ZnPc) /Zn-free phthalocyanine (H_2Pc) play the role of donors. Our results on the electronic structure show that the interaction between the $Sc_3N@C_{80}$ fullerene and the zinc and metal free phthalocyanines are different. The ground state dipole moment of $Sc_3N@C_{80}$-H_2Pc dyad is much larger than that of $Sc_3N@C_{80}$-ZnPc. The values of the lowest CT excitation energies for the two complexes differ by 0.3 eV. This is in contrast to the results obtained with C_{60} and C_{70} fullerenes with ZnTPP and TPP where the choice of acceptor component rather than the donor i.e. C_{60} vs. C_{70} produced larger effects on the CT energies. Overall, the role of the metal center is pronounced in the phthalocyanine based compounds. Considering other factors like the ionization potentials and exciton binding energies, a better performance may be expected for the $Sc_3N@C_{80}$-ZnPc dyad.

CONFICTS OF INTEREST

There is no conflict to declare.

ACKNOWLEDGMENT

This work was funded by the DOE Basic Energy Science under awards DE-SC0006818 and DE-SC0002168. Authors acknowledge the Texas Advanced Computing Center (TACC) from the National Science Foundation (NSF) (Grant No. TG-DMR090071) for computational time.

REFERENCES

1. L. Dou, Y. Liu, Z. Hong, G. Li and Y. Yang, *Chem. Rev.*, 2015, **115**, 12633.
2. Y. Li, *Acc. Chem. Res.*, 2012, **45**, 723.
3. K. Zhang, Z. Hu, C. Sun, Z. Wu, F. Huang and Y. Cao, *Chem. Mater.*, 2017, **29**, 141.
4. G. Zhang, K. Zhang, Q. Yin, X.-F. Jiang, Z. Wang, J. Xin, W. Ma, H. Yan, F. Huang and Y. Cao, *J. Am. Chem. Soc.*, 2017, **139**, 2387.
5. D. Deng, Y. Zhang, J. Zhang, Z. Wang, L. Zhu, J. Fang, B. Xia, Z. Wang, K. Lu, W. Ma and Z. Wei, *Nat. Commun.*, 2016, **7**, 13740.
6. M. Li, K. Gao, X. Wan, Q. Zhang, B. Kan, R. Xia, F. Liu, X. Yang, H. Feng, W. Ni, Y. Wang, J. Peng, H. Zhang, Z. Liang, H.-L. Yip, X. Peng, Y. Cao and Y. Chen, *Nat. Photonics*, 2016, **11**, 85.
7. J. Zhao, Y. Li, G. Yang, K. Jiang, H. Lin, H. Ade, W. Ma and H. Yan, *Nat. Energy*, 2016, **1**, 15027.
8. L. J. A. Koster, S. E. Shaheen and J. C. Hummelen, *Adv. Energy Mater.*, 2012, **2**, 1246.
9. C. J. Brabec, A. Cravino, D. Meissner, N. S. Sariciftci, T. Fromherz, M. T. Rispens, L. Sanchez and J. C. Hummelen, *Adv. Funct. Mater.*, 2001, **11**, 374.
10. M. C. Scharber, D. Mühlbacher, M. Koppe, P. Denk, C. Waldauf, A. J. Heeger and C. J. Brabec, *Adv. Mater.*, 2006, **18**, 789.
11. D. Veldman, S. C. J. Meskers and R. A. J. Janssen, *Adv. Funct. Mater.*, 2009, **19**, 1939.
12. K. Vandewal, A. Gadisa, W. D. Oosterbaan, S. Bertho, F. Banishoeib, I. Van Severen, L. Lutsen, T. J. Cleij, D. Vanderzande and J. V. Manca, *Adv. Funct. Mater.*, 2008, **18**, 2064.
13. T. Kietzke, D. A. M. Egbe, H.-H. Hörhold and D. Neher, *Macromolecules*, 2006, **39**, 4018.
14. V. Lemaur, M. Steel, D. Beljonne, J.-L. Brédas and J. Cornil, *J. Am. Chem. Soc.*, 2005, **127**, 6077.

15. A. A. Popov, S. Yang and L. Dunsch, *Chem. Rev.*, 2013, **113**, 5989.
16. L. Dunsch and S. Yang, *Small*, 2007, **3**, 1298.
17. J. M. Campanera, C. Bo, M. M. Olmstead, A. L. Balch and J. M. Poblet, *J. Phys. Chem. A*, 2002, **106**, 12356.
18. C. M. Cardona, B. Elliott and L. Echegoyen, *J. Am. Chem. Soc.*, 2006, **128**, 6480.
19. S. Stevenson, G. Rice, T. Glass, K. Harich, F. Cromer, M. R. Jordan, J. Craft, E. Hadju, R. Bible, M. M. Olmstead, K. Maitra, A. J. Fisher, A. L. Balch and H. C. Dorn, *Nature*, 1999, **401**, 55.
20. R. B. Ross, C. M. Cardona, D. M. Guldi, S. G. Sankaranarayanan, M. O. Reese, N. Kopidakis, J. Peet, B. Walker, G. C. Bazan, E. Van Keuren, B. C. Holloway and M. Drees, *Nature Materials*, 2009, **8**, 208.
21. R. B. Ross, C. M. Cardona, F. B. Swain, D. M. Guldi, S. G. Sankaranarayanan, E. Van Keuren, B. C. Holloway and M. Drees, *Adv. Funct. Mater.*, 2009, **19**, 2332.
22. J. R. Pinzón, M. E. Plonska-Brzezinska, C. M. Cardona, A. J. Athans, S. S. Gayathri, D. M. Guldi, M. A. Herranz, N. Martín, T. Torres and L. Echegoyen, *Angew. Chem., Int. Ed.*, 2008 **47**, 4173.
23. J. R. Pinzón, D. C. Gasca, S. G. Sankaranarayanan, G. Bottari, T. Torres, D. M. Guldi and L. Echegoyen, *J. Am. Chem. Soc.*, 2009, **131**, 7727.
24. L. Feng, S. Gayathri Radhakrishnan, N. Mizorogi, Z. Slanina, H. Nikawa, T. Tsuchiya, T. Akasaka, S. Nagase, N. Martín and D. M. Guldi, *J. Am. Chem. Soc.*, 2011, **133**, 7608.
25. B. Liu, H. Fang, X. Li, W. Cai, L. Bao, M. Rudolf, F. Plass, L. Fan, X. Lu and D. M. Guldi, *Chem. – Eur. J.*, 2015, **21**, 746.
26. Y. Takano, *Fullerenes, Nanotubes, Carbon Nanostruct.*, 2014, **22**, 243.
27. S. Wolfrum, J. R. Pinzón, A. Molina-Ontoria, A. Gouloumis, N. Martin, L. Echegoyen and D. M. Guldi, *Chem. Commun.*, 2011,47, **47**, 2270.
28. Y. Takano, M. Á. Herranz, N. Martín, S. G. Radhakrishnan, D. M. Guldi, T. Tsuchiya, S. Nagase and T. Akasaka, *J. Am. Chem. Soc.*, 2010, **132**, 8048.
29. W. Seitz, A. J. Jimenez, E. Carbonell, B. Grimm, M. S. Rodriguez-Morgade, D. M. Guldi and T. Torres, *Chem. Commun.*, 2010, **46**, 127.
30. L. Sanchez, N. Martin and D. M. Guldi, *Angew. Chem., Int. Ed.*, 2005, **44**, 5374.
31. K. Maurer, B. Grimm, F. Wessendorf, K. Hartnagel, D. M. Guldi and A. Hirsch, *Eur. J. Org. Chem.*, 2010, 5010.

32. B. Grimm, E. Karnas, M. Brettreich, K. Ohta, A. Hirsch, D. M. Guldi, T. Torres and J. L. Sessler, *J. Phys. Chem. B*, 2010, **114**, 14134.
33. H. Isla, B. Grimm, E. M. Pérez, M. Rosario Torres, M. Ángeles Herranz, R. Viruela, J. Aragó, E. Ortí, D. M. Guldi and N. Martín, *Chem. Sci.*, 2012, **3**, 498.
34. I. Sánchez-Molina, B. Grimm, R. M. Krick Calderon, C. G. Claessens, D. M. Guldi and T. Torres, *J. Am. Chem. Soc.*, 2013, **135**, 10503.
35. B. Grimm, J. Schornbaum, C. M. Cardona, J. D. van Paauwe, P. D. W. Boyd and D. M. Guldi, *Chem. Sci.*, 2011, **2**, 1530.
36. A. J. Jimenez, B. Grimm, V. L. Gunderson, M. T. Vagnini, S. Krick Calderon, M. S. Rodriguez-Morgade, M. R. Wasielewski, D. M. Guldi and T. Torres, *Chem. – Eur. J.*, 2011, **17**, 5024.
37. D. M. Guldi, J. Ramey, M. V. Martínez-Díaz, A. D. L. Escosura, T. Torres, T. Da Ros and M. Prato, *Chem. Commun.*, 2002, 2774.
38. D. M. Guldi, A. Gouloumis, P. Vázquez and T. Torres, *Chem. Commun.*, 2002, 2056.
39. Y. Takano, S. Obuchi, N. Mizorogi, R. García, M. Á. Herranz, M. Rudolf, D. M. Guldi, N. Martín, S. Nagase and T. Akasaka, *J. Am. Chem. Soc.*, 2012, **134**, 19401.
40. M. Rudolf, L. Feng, Z. Slanina, T. Akasaka, S. Nagase and D. M. Guldi, *J. Am. Chem. Soc.*, 2013, **135**, 11165.
41. L. Feng, M. Rudolf, S. Wolfrum, A. Troeger, Z. Slanina, T. Akasaka, S. Nagase, N. Martín, T. Ameri, C. J. Brabec and D. M. Guldi, *J. Am. Chem. Soc.*, 2012, **134**, 12190.
42. L. Feng, M. Rudolf, O. Trukhina, Z. Slanina, F. Uhlik, X. Lu, T. Torres, D. M. Guldi and T. Akasaka, *Chem. Commun.*, 2015, **51**, 330.
43. O. Trukhina, M. Rudolf, G. Bottari, T. Akasaka, L. Echegoyen, T. Torres and D. M. Guldi, *J. Am. Chem. Soc.*, 2015, **137**, 12914.
44. I. Bruder, J. Schöneboom, R. Dinnebier, A. Ojala, S. Schäfer, R. Sens, P. Erk and J. Weis, *Organic Electronics*, 2010, **11**, 377.
45. S. Wolfrum, J. R. Pinzo´, A. Molina-Ontoria, A. Gouloumis, N. Martı´, L. Echegoyen and D. M. Guldi, *Chem. Commun.*, 2011, **47**, 2270.
46. S. Fukuzumi, K. Onkubi, and T. Suenobo, Acc. Chem. Res., 2014, **47**,1455.
47. R. C. Huber, A. S. Ferreira, R. Thompson, D. Kilbride, W. S. Knutson, L.S. Devi, D. B. Toso, J. R. Challa, Z. H. Zhou, Y. Rubin, B. J. Schwartz, S. H. Tolbert, Science, 2015, 348, 1340.

48. K. Kimoto, T. Satoh, M. Iwamura, K. Nozaki, T. Horikoshi, S. Suzuki, M. Kozaki, K. Okada, J. Phys. Chem. A, 2016, 120, 8093.
49. Regina J. Hafner, Liangfei Tian, Jan C. Brauer, Thomas Schmaltz, Andrzej Sienkiewicz, Sandor Balog, Valentin Flauraud, Juergen Brugger, and Holger Frauenrath, ACS Nano Article ASAP, DOI: 10.1021/acsnano.8b031
50. L. Basurto, F. Amerikheirabadi, R. Zope and T. Baruah, *Phys. Chem. Chem. Phys.*, 2015, **17**, 5832.
51. F-R. Fan and L. R. Faulkner, J. Chem. Phys., 1978, 69, 3334.
52. R. O. Loutfy and J. H. Sharp, J. Chem. Phys., 1979, 71, 1211.
53. K. Suemori, T. Miyata, M. Hiramoto, M. Yokoyama, Japan. J. Appl. Phys. 2004, 43, L1014.
54. Masayuki Kubo, Yusuke Shinmura, Norihiro Ishiyama, Toshihiko Kaji & Masahiro Hiramoto, Molecular Crystals and Liquid Crystals, 2013, 581:1, 13-17, DOI: 10.1080/15421406.2013.808137.
55. J. P. Perdew, K. Burke and M. Ernzerhof, *Phys. Rev. Lett.*, 1996, **77**, 3865.
56. M. R. Pederson, D. V. Porezag, J. Kortus and D. C. Patton, *Phys. Status Solidi B*, 2000, **217**, 197.
57. M. R. Pederson and K. A. Jackson, *Phys. Rev. B* 1990, **41**, 7453.
58. M. R. Pederson and K. A. Jackson, *Phys. Rev. B*, 1991, **43**, 7312.
59. K. A. Jackson and M. R. Pederson, *Phys. Rev. B*, 1990, **42**, 3276.
60. T. Cai, C. Slebodnick, L. Xu, K. Harich, T. E. Glass, C. Chancellor, J. C. Fettinger, M. M. Olmstead, A. L. Balch, H. W. Gibson and H. C. Dorn, *J. Am. Chem. Soc.*, 2006, **128**, 6486.
61. D. Porezag and M. R. Pederson, *Phys. Rev. A*, 1999, **60**, 2840.
62. S. Grimme, J. Antony, S. Ehrlich and H. Krieg, *J. Chem. Phys.*, 2010, **132**, 154104.
63. T. Baruah and M. R. Pederson, *J. Chem. Theory Comput.*, 2009, **5**, 834.
64. T. Baruah, M. Olguin and R. R. Zope, *J. Chem. Phys.*, 2012, **137**, 084316.
65. R. R. Zope, M. Olguin and T. Baruah, *J. Chem. Phys.*, 2012, **137**, 084317.
66. M. Olguin, R. R. Zope and T. Baruah, *J. Chem. Phys.*, 2013, **138**, 074306.
67. R. S. Mulliken, *J. Phys. Chem.*, 1952, **56**, 801.
68. G. Ruani, C. Fontanini, M. Murgia and C. Taliani, *J. Chem. Phys.*, 2002, **116**, 1713.
69. B. Kessler, *Applied Physics A*, 1998, **67**, 125.
70. I. N. Ioffe, A. S. Ievlev, O. V. Boltalina, L. N. Sidorov, H. C. Dorn, S. Stevenson and G. Rice, *Int. J. Mass Spectrom.*, 2002, **213**, 183.

71. J. Berkowitz, *J. Chem. Phys.*, 1979, **70**, 2819.
72. A. Gouloumis, S.-G. Liu, Á. Sastre, P. Vázquez, L. Echegoyen and T. Torres, *Chem. – Eur. J.*, 2000, **6**, 3600.
73. Y. Zhu, Y. Li and Z. Q. Yang, *Chem. Phys. Lett.*, 2008, **461**, 285.
74. T. Ziegler, A. Rauk and E. J. Baerends, *Theoret. China. Acta*, 1977, **43**, 261.
75. M. Krause, and L. Dunsch, ChemPhysChem, 2004, **5**, 1445-1449.
76. T. Nojiri, M. M. Alam, H. Konami, A. Watanabe and O. Ito, *J. Phys. Chem. A*, 1997, **101**, 7943.